Original Research Article

Long term follow-up of pCO_2, pCH_4 and emissions from Eastmain 1 boreal reservoir, and the Rupert diversion bays, Canada

Maud Demarty [a,*], Alain Tremblay [b]

[a] Englobe Corp., 1001, rue Sherbrooke Est, Montréal, Québec H2L 1L3, Canada
[b] Hydro-Québec, 75, boul. René-Lévesque Ouest, Montréal, Québec H2Z 1A4, Canada

ABSTRACT

Eastmain 1 reservoir (James Bay area, Quebec, Canada) is a 600 km^2 boreal reservoir, created in November 2005 in the Eastmain River watershed. To increase the volume of water transiting in Eastmain 1 (EM 1), the Rupert River was diverted. Partial flooding of the Rupert diversion bays (RD) took place in 2009 and the flooding was completed in 2011. CO_2 and CH_4 partial pressures and emissions were monitored for 7 years on the reservoir and bays.

According to field campaigns measurements at Eastmain-1 reservoir, average ice-free period pCO_2 varied between 969 μatm and 2230 μatm, whereas the average pCO_2 of the reference sampled lakes and Eastmain River stations was 592 μatm ($\pm$101) before the impoundment. Contrary to pCO_2, pCH_4 partial pressures presented any pattern to outline after flooding of the Eastmain 1 reservoir and varied between 21 and 250 μatm, with an overall average of 106 μatm (SD $\pm$ 91). CO_2 diffusive emissions at the air–water interface of the Eastmain-1 reservoir ranged between −113 mg C-CO_2 m^{-2} day^{-1} and 8237 mg C-CO_2 m^{-2} day^{-1}. CH_4 fluxes ranged from null to 102 mg C-CH_4 m^{-2} day^{-1}. This article also shows that the impoundment of the Rupert River and the related transport of sediment and organic matter into Eastmain 1 Reservoir did not have a significant long term effect on $pCO2$.

Remarkably, the different approaches/methods used to monitor these variables showed comparable results: a net decrease in CO_2 emissions in the first three years followed by stabilization around seven years after the reservoir creation. Therefore, we advocate for long-term, around 10 years, GHG monitoring. The use of various methods, beforehand intercalibrated, offers a non-negligible flexibility, reducing the sampling costs, which should favor an increase in this kind of studies worldwide.

© 2017 European Regional Centre for Ecohydrology of the Polish Academy of Sciences. Published by Elsevier Sp. z o.o. All rights reserved.

1. Introduction

Lakes, rivers, wetlands and reservoirs are sources of greenhouse gases (GHGs) (Kortelainen et al., 2000; Tremblay et al., 2005; Cole et al., 2007). The greenhouse effect is crucial for life on earth as it contributes to maintain a mean annual temperature of about 15 °C (Lindsey, 2009). However, over the last two decades, the rate of increase of anthropogenic GHG emissions to the atmosphere has reached a critical level. The major GHGs related to the creation of reservoirs are carbon dioxide (CO_2), methane (CH_4) and nitrous oxide (N_2O) (Eggleston et al., 2006). Geography, water residence time, reservoir shape and volume, and amount and type of vegetation flooded are variables that affect the duration and quantity of emissions (St Louis et al., 2000; Barros et al., 2011;

* Corresponding author.
  E-mail address: maud.demarty@englobecorp.com (M. Demarty).

Tremblay et al., 2005). In Canada, hydropower plants represent about 65% of the electricity generation capacity (National Energy Board, 2010); among them, run-of-the-river plants do not present significant GHGs emissions and plants with reservoirs have low GHG emissions, in the order of 35–70 times less GHGs per terawatt-hour than thermal power plants, N_2O emissions being negligible (Tremblay et al., 2005). Nevertheless, in regards to climate change, the contribution of freshwater reservoirs to the increase of GHGs in the atmosphere is of growing concern (e.g., St Louis et al., 2000; Rudd et al., 1993) for government and the energy sectors, as erosion and sediment transport due to intense storm events and water pollution increase worldwide.

CO_2 and CH_4 production in aquatic systems is fueled by inputs from the watershed (Marchand et al., 2009; Campeau et al., 2014). These processes can lead to CO_2 supersaturation in the water column (Del Giorgio et al., 1999; Duarte and Prairie, 2005) and/or CH_4 accumulation in the sediments, and thus produce gas emission to the atmosphere through diffusion at the water surface (Kling et al., 1992; MacIntyre et al., 1995) and bubbling (Deshmukh et al., 2014). In hydroelectric reservoirs, greenhouse gases (GHGs) can be emitted by three main pathways, the two first being also observed in natural waterbodies: diffusive emissions at the reservoir surface (Huttunen et al., 2003; Abril et al., 2005), bubbling (mostly in shallow areas, Huttunen et al., 2003; Rosa et al., 2002), and downstream emissions comprising degassing in the turbulent waters up to 1 km downstream the dam (Roehm and Tremblay, 2006), and diffusive and bubble emissions in the river up to 50 km downstream the dam. In Canada, preliminary results showed that bubbling was of minor extent compared to diffusive emissions (Bastien et al., 2010). Degassing estimates are under study (unpublished data). Here, we thus focused on diffusive fluxes.

According to the available studies on young and old reservoirs worldwide, the magnitude of CO_2 diffusive emissions is related to the reservoirs age and latitude (Barros et al., 2011). Typically, the largest amount of GHG emissions takes place during the first 10 years after flooding for boreal (Tremblay et al., 2005; Marchand et al., 2012) as well as for tropical reservoirs (Abril et al., 2005; Demarty and Bastien, 2011). After the first 10 years, CO_2 emissions are similar to those from natural aquatic systems in the same watershed. Such a clear pattern is not observed for CH_4 as organic matter mineralization in CH_4 is highly dependent of the hypolimnetic oxygen concentration (Clayer et al., 2016) and CH_4 bubbling is also related to sedimentation rate and its nature (DelSontro et al., 2010).

Several methods can be used to monitor emissions before and after a reservoir creation, such as floating chambers, automated systems, eddy covariance towers (UNESCO/IHA, 2010). Some studies confirmed the reliability of different techniques used to measure the same processes (Demarty et al., 2009; Deshmukh et al., 2014; Zhao et al., 2015); some other studies demonstrated disparities between methods (Vachon et al., 2010). The need of new data about GHG emissions from reservoir is recognized worldwide for novel insights and better understanding of the processes involved. Hence, the main objective of the present article is to present new dataset on GHG emissions from reservoir, considering the use of recognized approaches and methods. However, the quality, the temporal and spatial distribution of our data and the different methods used in our follow-up allowed robust analysis of the technologies and approaches in one hand, and of the pattern of GHG concentrations and emissions in the other hand. These analyses were based on the following hypothesis. In 2009, Demarty et al. reported a matching between trends stemming from measurements made either with automated systems in generating station or during discrete field campaigns for the first years after impoundment. We hypothesize this concordance to be valuable for the entire study period. In 2012, Teodoru et al. presented the decreasing trend in CO_2 emissions at the Eastmain-1 reservoir from its impoundment in 2005–2009. According to their results, we expected CO_2 emissions for the 2009–2012 period to be much lower. However, the impoundment of the Rupert bays upstream the Eastmain 1 Reservoir in 2010 represented an important input of organic matter in the reservoir. It was then hypothesized that this event led to an increase in surface CO_2 and CH_4 partial pressures in the Eastmain-1 reservoir.

2. Material and methods

2.1. Study area

Eastmain 1 reservoir (52.19° N 75.05° W; Fig. 1A) is located in the boreal zone, northwestern Québec, Canada. Within this region, mean monthly temperatures vary between −23 °C and 14 °C, and total rainfall and total snow precipitation are up to 430 mm and 260 mm, respectively. The Eastmain River's catchment (25,857 km^2) is dominated by coniferous forest, shallow podzolic and peat soils, and igneous bedrock. The aquatic system studied is oligotrophic, with an overall low primary production (Planas et al., 2005). The reservoir is partially to totally covered by ice from about 15 December to 15 May (according to Hydro-Québec surveys).

Eastmain 1 reservoir (603 km^2) was flooded in November 2005 and the generating station (480 MW) was commissioned in 2006. The Eastmain-1-A-Sarcelle-Rupert Project aimed to give Hydro-Québec's generating fleet additional capacity of 918 MW and additional output of 8.7 TWh per year. It implied an increase in the volume of the Eastmain 1 reservoir and by diverting the Rupert River. Partial flooding of the Rupert River diversion (RD) started in 2009 with the upstream bay (229 km^2) and the flooding was completed in 2011 in the downstream bay (118 km^2; Fig. 1C). The RD bays flow into the southeast section of Eastmain 1 reservoir (600 $m^3 s^{-1}$). The zone of sedimentation at the point of entry into the reservoir is presented in Fig. 1B. This map also presents GHG sampling stations in this specific area.

Sampling dates between 2005 (so-called reference lakes and river sampled before reservoir creation) and 2012 and the number of sampling stations (visited once per sampling period) are described in Table 1. Sampling strategy regarding the spatial variability and sampling
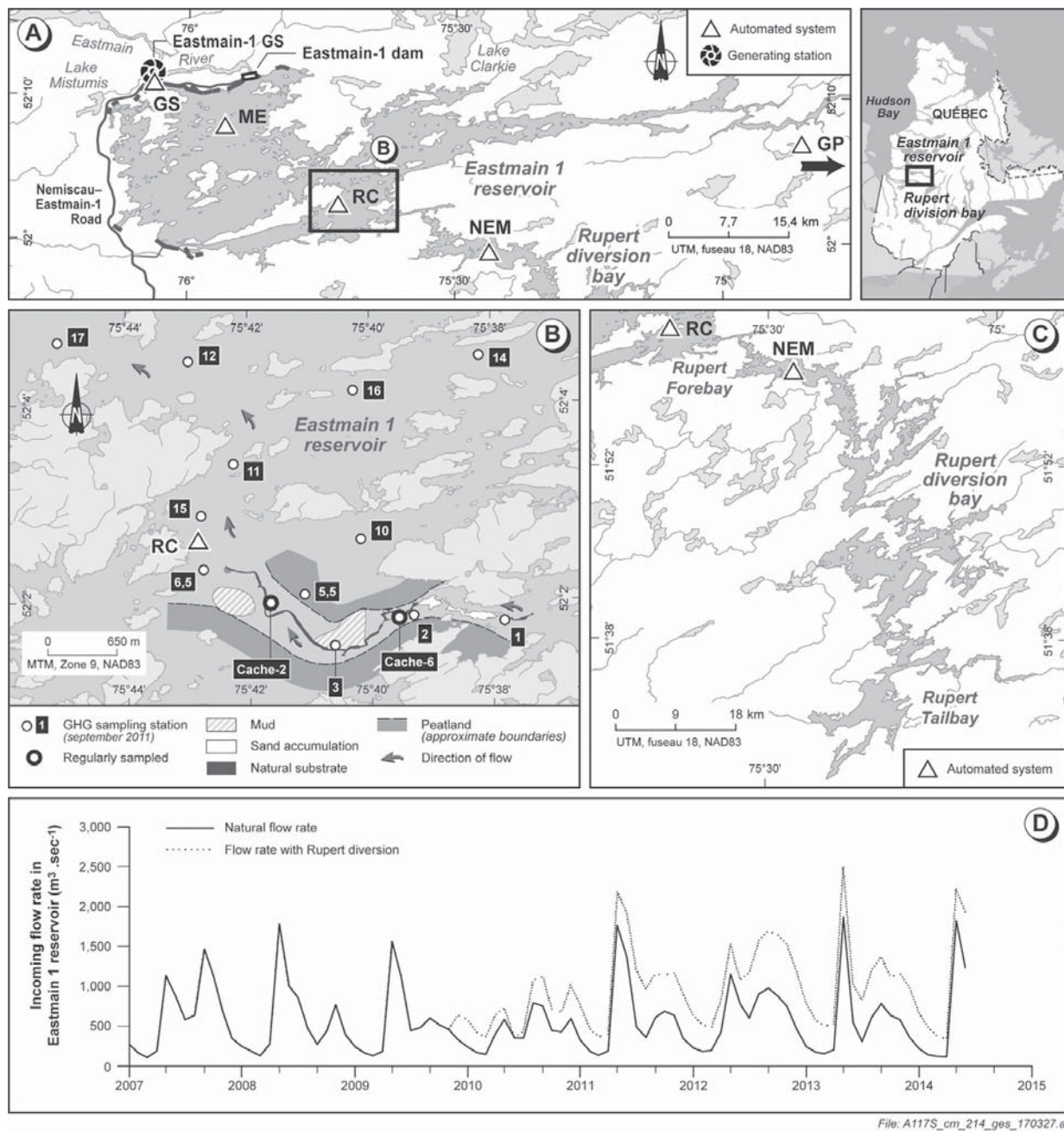
Fig. 1. Eastmain 1 study area with continuous GHG sampling stations (A), focus on the sediment fan area of the Rupert diversion as it enters Eastmain 1 reservoir (B), Rupert study area with continuous GHG sampling (C) and flow rate entering the Eastmain 1 reservoir (D).

stations location for the field campaigns are described in Demarty et al. (2011).

2.2. Field campaigns CO_2 and CH_4 partial pressures measurements and fluxes calculation

The partial pressure of CO_2 and CH_4 (pCO_2 and pCH_4) was measured at the water surface (0.1 m) for all sampling stations at Eastmain 1 reservoir. To measure pCO_2, water was sampled with a peristaltic pump and surface water pCO_2 was measured in situ with a non-dispersive infrared (NDIR) sensor (EGM-4 manufactured by PP Systems) coupled with a gas exchanger (Membrana Celgard). Ten

consecutive measurements (one per minute) were averaged to obtain the pCO_2 at each station (mean variation coefficient of 1.3%). Due to technical improvement with time, different sensors/techniques were used for pCH_4 measurements. Head-space technique and chromatography (flame ionization detector; Demarty et al., 2011) were used in 2006, 2007, 2008 and 2010. Peristaltic pump and gas exchanger setup (as for pCO_2) coupled with a Tunable Diode Laser Spectroscopy sensor (TDLS manufactured by Franatech) were used in 2009, 2011 and 2012. CO_2 and CH_4 dissolve concentrations were calculated according to Demarty et al. (2011). Diffusive fluxes were then calculated according to Thin Boundary Layer (TBL) model and

Table 1
Sampling periods and number of sampling stations in the study area.

Sampling year	Winter field campaigns		Summer field campaigns			Autumn field campaigns	
	Dates	Number of stations	Dates	Number of stations Eastmain 1 Reservoir	Number of stations Rupert Bays	Dates	Number of stations
2005			Jul., 23 to Aug. 10	29			
2006			Jul., 10–22	41		Sept., 18 to Oct., 4	42
2007	Mar., 20–28	39	Jul., 5–21	38	34		
2008	Jan., 14–26 and Mar. 26 to Apr. 5	42/35	Jul., 3–22	57	36	Sept., 15–22	27
2009			Jul., 17 to Aug. 1st		36		
2010			Jul., 3–23	16	35		
2011			Jul., 27 to Aug. 16	29	40	Sept., 5–10	20
2012			Jul., 31 to Aug. 16	32	39		

estimates of k_{600} from Vachon and Prairie (2013) (model C). These authors argue for a better predictive model when using lake area together with wind speed, which we measured. Also considering that wind speed to k_{600} relationships are site-specific and that the majority of Vachon and Prairie's samples came from Eastmain 1 reservoir, this equation was the most suitable to our study.

2.3. CO_2 and CH_4 surface diffusive fluxes measurement

Point-in-time diffusive flux measurements were made using a floating chamber (FC). This method is known to overestimate the fluxes due to excess turbulence created by the chamber (MacIntyre et al., 1995; Vachon et al., 2010). For technical reasons, turbulences were not measured concomitantly to fluxes and therefore not taken into account to correct fluxes accordingly. In 2008, the gas collection chamber was rectangular, made of plastic, has an area of $0.20\,m^2$ and a volume of 18 L. The subsequent years, the chamber was improved, with a tapered shape, heavier structure for better stability (aluminum and fixed buoys), but similar area ($0.16\,m^2$) and volume (17.6 L). In both cases, the chamber walls extended 15 cm under water, thus ensuring a tight seal between the chamber and the water. Usually, the chamber was ventilated 5 min before the flux measurement begins, until the air GHG concentration measured by the gas analysers stabilizes and was comparable to that in the atmosphere (approximately $385\,\mu atm$ for CO_2 and $1.8\,\mu atm$ for CH_4, measured in the study area). After the chamber was set on the water surface, the internal pressure was equalized with that of the atmosphere by means of a port positioned on top of the chamber. This port was hermetically sealed with a rubber stopper at the beginning of the flux measurement. An external pump circulates air between the chamber and the gas analysers. A flow meter allows the circuit air flow to be controlled at $2.8\,L\,min^{-1}$.

Over the years, for technical reasons, GHG fluxes were measured using different sensors coupled in closed circuit to the floating collection chamber. CO_2 and CH_4 diffusive emissions were measured using a Gasmet DX4010 (Fourier Transform Infra Red sensor) in 2006 and 2007. In 2008 and 2009, only CO_2 emissions were measured using a PPSystems Ciras-SC (Non Dispersive Infra Red sensor).

Finally, from 2010 to 2012, CO_2 and CH_4 diffusive emissions were measured using a Picarro G1301. In any case, the flux measurement was carried out over a period of 7 min, during which the CO_2/CH_4 partial pressure trapped under the chamber was constantly recorded. The linear regression slope was used to calculate a GHG flux (in $mgCO_2\,m^{-2}\,day^{-1}$ or in $mgCH_4\,m^{-2}\,day^{-1}$) representing a GHG quantity emitted or collected per area and time unit, using the following equation:

$$\text{Flux} = \text{slope} \times F1 \times F2 \times \frac{\text{volume}}{\text{area}}$$

where $F1$ is a conversion factor from μatm to $mg\,m^{-3}$ for normal temperature and pressure conditions ($25\,°C$ and $101.3\,kPa$), $F2$ is a conversion factor of seconds on a daily basis, and the volume and area are those of the floating chamber. Three replicates were measured per sampling station.

2.4. Continuous CO_2 and CH_4 partial pressures measurements with automated systems

The continuous gas monitor was developed by Fisheries and Oceans Canada, in conjunction with Manitoba Hydro, after Carignan's design (1998) and built of commercial components. Every three hours, CO_2 and CH_4 are measured by two different sensors (LICOR LI-820 NDIR sensor and Neodym Panterra metal oxide semiconductor sensor, respectively) on a gas stream that has been equilibrated with the source water (Demarty et al., 2009). Long term partial pressure measurements taken at a single sampling station with monitors installed in GS have been shown to give conservative (compared to point-in-time measurements with floating chambers) and representative estimates of GHG fluxes for the whole reservoir (Québec and Manitoba, Demarty et al., 2009).

Automated GHG systems (monitors; AS) have been in place at Eastmain-1 generating station (GS) since 2006 to obtain CO_2 and CH_4 partial pressure time series. Since June 2007, and for the ice-free period (June to October), two AS were installed on rafts. The AS located in the Eastmain River upstream the reservoir (Gorge Prospere, GP in Fig. 1) was representative of the partial pressures entering the

reservoir. The second AS was installed in the center of the reservoir (Marie-Eve; ME in Fig. 1). Since June 2010, and for the ice-free period, two additional rafts with AS were installed at the entrance of the Rupert diversion into Eastmain 1 reservoir. The AS at Nemiscau (NEM) was dedicated to the outflow from the Rupert Diversion, whereas AS at Ruisseau Caché (RC) was at the confluence of the two water bodies.

2.5. Ancillary water quality measurements

Each sampling station was located according to a GPS, Garmin WGS 84. Total depth at the sampling stations was measured with a depth meter, Digital Hondex. Water column transparency was estimated with a Secchi disc. Atmospheric pressure, air temperature and wind speed were measured with a portative weather station, Kestrel Extech Instruments 407112. Surface and profiles for water temperature, pH and dissolved oxygen concentration were measured with a YSI 600XL. Alcalinity was measured with a pH meter, Thermo Orion Tree Stars 8102 BNWP.

3. Results and discussion

3.1. General observations at the Eastmain 1 reservoir

Surface water quality (transparency, temperature, pH, alkalinity, dissolve oxygen saturation) and meteorological (wind speed, air temperature) parameters measured for 6 years at Eastmain 1 Reservoir are presented in Table 2 (means and standard deviations). A significant increase in transparency was observed from 2006 to 2011 (Anova and Tukey–Kramer, $p < 0.05$). Concomitantly, pH increased (Anova and Tukey–Kramer, $p < 0.05$); as expected, this trend in pH was related to decrease in pCO_2, however the weakness of the relationship tend to demonstrate that pH measured on the field (in situ YSI probe) is not sensitive enough to be used as a proxy for pCO_2 estimation (regression, $p < 0.05$, $R^2 = 0.47$). The entire system is well oxygenated, apart from two stations that experienced O_2 depletion in the first spring after flooding (April 2008): concentrations of 3.1 and 3.2 mg L^{-1} were measured compared to an average of 10.0 ± 1.1 mg L^{-1} for the 34 other stations monitored at the same period.

Summertime sampling showed a stratification of the reservoir (for stations deeper than 8 m) with low O_2 and high CO_2 concentrations at the bottom. Autumnal sampling did not show this stratification, confirming that the water column mixing occurred before our autumnal campaigns. As lakes and rivers, the Eastmain 1 reservoir was supersaturated in CO_2 for the entire study period. Hydrometric follow-up showed two flood events per year (Fig. 1D), in spring and fall. They represent organic matter inputs that surely sustained the heterotrophic mode of the system and favored the CO_2 supersaturation. Indeed, Berggren et al. (2012) demonstrated that in heterotrophic systems, the respiratory quotient (moles of CO_2 produced per mole of O_2 consumed) of the bacterioplankton was higher than in autotrophic systems. Hence, allochtonous organic matter entering the system twice a year leads to

more CO_2 per O_2 consumed than would have done organic matter produced by the algal community of the reservoir.

3.2. Temporal trends in pCO_2 in Eastmain 1 Reservoir

Results from year-round pCO_2 monitored with an AS installed in Eastmain 1 generating station (GS) are presented in Fig. 2A and measurements from field campaigns are presented in Fig. 2B. As stated in Demarty et al. (2009), measurements made on the water passing through the turbines should be representative of the whole reservoir. In that article, authors presented conclusions from one year measurement at Eastmain 1 reservoir and several years of measurements in Manitoba reservoirs. The multi-annual datasets presented in this article tend to confirm their observations. Trends depicted from 2006 to 2012 AS results are similar to those from field campaigns measurements for the same period. The advantage of the AS is clearly to get a year-round dataset, which is not feasible with field campaigns that cannot be performed in spring and late autumn for security reasons (ice break-up or formation).

pCO_2 trends can be described as follow: first, pCO_2 increase under ice-cover (Demarty et al., 2011; Huttunen et al., 2004) is clearly demonstrated every year with the highest peak in pCO_2 observed the first winter after impoundment (2007). Winter field campaigns performed in 2007 and 2008 corroborate AS measurements. In case of
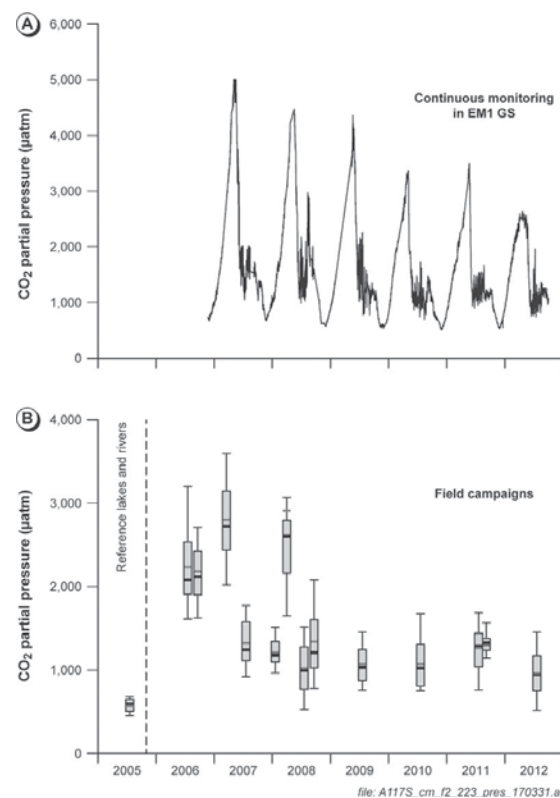

Fig. 2. CO_2 partial pressures monitored using an automated system installed in the Eastmain 1 generating station (A) or measured from 2005 to 2012 at many sampling stations during field campaigns (B). Box represents 75th percentiles error bars represent 10th and 90th percentiles, gray bar represents mean and full line represents median.

Table 2
Mean water quality parameters measured during field campaigns conducted in the future Eastmain 1 reservoir area in 2005 and on the Eastmain 1 Reservoir from 2006 to 2012. For number of samples/stations, refer to Table 1.

Sampling year	Sampling season	Water transparency (m)		Surface water temperature (°C)		Surface pH		Surface alkalinity (mg L^{-1} CaCO$_3$)		Surface oxygen saturation (%)		pCO$_2$ (μatm)		pCH$_4$ (μatm)		Air temperature (°C)		Wind speed (m s^{-1})	
		Mean	SD	Mean	SD	Mean	SD	Mean	SD	Mean	SD	Mean	SD	Mean	SD	Mean	SD	Mean	SD
2005	Summer	2.0	0.7	16.8	1.4	6.66	0.32	3.29	1.67	99.0	6.3	592	101	N.A.	N.A.	16.0	2.7	3.5	1.4
2006	Summer	1.9	0.3	17.8	1.4	5.95	0.13	3.05	0.57	83.0	6.4	2181	485	125	153	19.7	3.0	2.6	1.8
	Autumn	1.7	0.2	11.3	1.1	5.98	0.19	1.57	0.90	77.3	6.5	2230	563	83	65	9.2	2.4	3.7	1.3
2007	Late Winter	N.A.	N.A.	0.1	0.2	5.78	0.19	2.42	0.56	80.8	10.1	2798	708	20	31	N.A.	N.A.	N.A.	N.A.
	Summer	2.0	0.2	15.4	2.0	6.10	0.30	1.85	0.65	92.7	6.1	1333	317	N.A.	N.A.	17.1	3.1	2.6	1.2
2008	Winter	N.A.	N.A.	0.1	0.0	6.10	0.29	2.03	0.62	92.7	5.3	1211	194	40	82	N.A.	N.A.	3.5	0.0
	Late Winter	N.A.	N.A.	0.2	0.2	5.94	0.16	2.58	0.81	67.2	13.1	2910	2415	306	1007	−6.2	6.2	3.5	1.6
	Summer	2.0	0.3	18.9	1.5	6.22	0.20	1.51	0.27	94.9	11.8	1025	361	58	57	18.2	3.3	2.8	1.2
	Autumn	2.0	0.2	12.1	2.6	6.17	0.27	1.71	0.38	82.4	6.7	1344	458	38	37	7.7	3.3	4.2	1.6
2009	Summer	2.1	0.3	17.8	1.1	6.19	0.12	1.62	0.32	94.6	4.1	1071	301	104	134	18.9	2.8	3.0	1.3
2010	Summer	1.9	0.4	18.9	1.0	N.A.	N.A.	N.A.	N.A.	89.3	8.8	1072	316	21	25	19.5	3.1	3.1	1.2
2011	Summer	2.6	0.5	18.9	0.6	6.59	0.14	3.53	1.70	82.2	7.5	1276	398	117	125	18.0	2.8	3.0	1.2
	Autumn	2.7	0.4	16.1	0.5	6.73	0.19	6.33	2.09	88.7	5.7	1297	203	258	198	12.6	3.1	3.8	1.5
2012	Summer	2.4	0.5	18.3	1.3	6.55	0.24	3.84	1.60	89.6	16.3	969	364	102	109	18.6	4.6	2.6	1.2

N.A.: not available.

Eastmain 1, under ice-cover pCO$_2$ increase observed is an indication of the degradation of in situ organic matter, as during winter, organic matter income from the watershed is relatively small (23% of the summer income in the main channel; incomes in dentritic parts of the reservoir are thus considered close to null; information form Hydro Québec hydrometric services, not shown). Secondly, springtime degassing linked to ice break-up is obvious. Measured pCO$_2$ at the end of this degassing phase decreased year after year (Anova and Tukey–Kramer, $p < 0.05$). This corresponds to a background pCO$_2$ for the ice-free period. Third, AS records showed that lowest pCO$_2$ values are reached at the end of autumn.

At Eastmain-1 reservoir, according to field campaigns measurements, average ice-free period pCO$_2$ varied between 969 μatm (summer 2012) and 2230 μatm (autumn 2006; Fig. 2 and Table 2). Before impoundment (2005), the average pCO$_2$ of the reference sampled lakes and Eastmain River stations was 592 μatm (±101). The averaged pCO$_2$ increased drastically after impoundment (2330 μatm in summer 2006) and decreased significantly the subsequent 2007 and 2008 summers. The difference in pCO$_2$ from 2008 to 2011 was insignificant and a drop occurred in 2012 (Anova and Tukey–Kramer, $p < 0.05$). In parallel to field campaigns data analysis, summer/autumn AS datasets were used to compute mean summer CO$_2$ partial pressures and concentrations from 2007 to 2012 (Table 3). The decreasing trend in pCO$_2$ observed through yearly field campaigns is confirmed with a significant decrease from summer 2007 to summer 2010. pCO$_2$ recorded by the AS at Eastmain-1 GS are generally higher than those measured during field campaigns; in fact, records in the GS are made on the integrated water column (whose highly depended on the water intake depth), whereas field campaigns data represented water surface measurements. As presented earlier, profiles conducted on

the reservoir showed that pCO$_2$ increased with depth, which supports these observations.

Since June 2007, the two automated systems installed upstream the reservoir (GP) and in a central station of the reservoir (ME) depicted ice free periods daily variations in pCO$_2$ (Table 4 and Fig. 3). Trends observed at GP represented the natural variation of the Eastmain River upstream the reservoir. At this location, pCO$_2$ varied from 455 (in 2010) to 1323 μatm (in 2009), but there was no specific trend over the years (see Table 4 for ice-free period average) and the overall averaged pCO$_2$ was 656 μatm (±127). Due to its location, the ME station was supposed to reflect the overall reservoir trends in pCO$_2$. Here again, a decrease in pCO$_2$ from 2007 to 2010 and highest values were recorded in 2011 (Anova and Tukey–Kramer, $p < 0.05$). pCO$_2$ recorded at this representative station of the reservoir were higher than those measured at GP, but lower than those measured (1) by the AS in the Eastmain 1 GS (which integrate the entire water column) and (2) during the field campaigns (spatial variation taken into account).

Interestingly, we demonstrated that three different approaches can be used to adequately depict major trends in pCO$_2$ in a reservoir. Considering the absolute values, pCO$_2$ values recorded in the GS were the highest (in average 1.8 times higher than the measurements made at Marie Eve AS station). Consequently, the monitoring method must be chosen carefully, considering the purpose of the study.

3.3. Temporal trends in pCH$_4$ in Eastmain 1 Reservoir

Contrary to pCO$_2$, pCH$_4$ partial pressures presented any pattern to outline after flooding of the Eastmain 1 reservoir. There was no significant difference among measurements gathered during ice free campaigns from 2006 to 2012 (Table 2). pCH$_4$ varied between 21 (measured in summer

Table 3

Ice free period pCO_2, CO_2 concentrations, surface fluxes and winter community respiration rates under ice-cover – calculations from pCO_2 monitored by the automated system installed in Eastmain-1 generating station.

Ice free period										Ice cover period	
Year	n	Mean pCO_2	SD	Mean [CO2]	SD	Tukey test result	Mean surface flux			Year	Winter CO_2 increase
				molC L^{-1}			mmolC L^{-1} day^{-1}	SD	Tukey test result		µmolC L^{-1} day^{-1}
2007	170	1380	343	66.2	12.4	a	142.8	110.6	a	2006–2007	1.5
2008	121	1472	512	66.3	19.0	a	158.6	111.6	a	2007–2008	1.5
2009	168	1136	167	55.0	16.7	b	130.8	121.3	a	2008–2009	1.3
2010	162	992	245	47.1	7.9	c	77.2	35.0	bc	2009–2010	1.1
2011	169	1064	235	49.5	6.9	c	53.4	28.0	c	2010–2011	0.9
2012	109	1083	144	47.7	6.9	c	95.8	48.8	b	2011–2012	0.8

Table 4

Means in pCO_2 and pCH_4 (in µatm) monitored by the automated system installed in Eastmain-1 generating station (GS, year-round), and on floating decks during ice-free periods on Eastmain River (GP), Eastmain 1 Reservoir (ME and RC) and Rupert bays outflow (NEM).

| Sampling year	GS (year-round)						GP (ice-free period)						ME (ice-free period)						RC (ice-free period)						NEM (ice-free period)					
	pCO_2	n	SD	pCH_4	n	SD	pCO_2	n	SD	pCH_4	n	SD	pCO_2	n	SD	pCH_4	n	SD	pCO_2	n	SD	pCH_4	n	SD	pCO_2	n	SD	pCH_4	n	SD
2006	815	39	97	23	39	11																								
2007	1986	362	1174	47	365	43	634	103	48	34	114	14	963	112	342	39	3	17												
2008	2005	317	1111	33	366	28	652	49	69	47	48	14	970	101	168	N.A.		N.A.												
2009	1693	350	962	35	365	26	692	49	230	19	48	21	920	66	136	79	65	79												
2010	1366	342	696	14	365	21	597	72	69	8	73	7	855	59	217	41	20	16	1460	90	280	220	90	317	1602	111	461	10	88	11
2011	1302	326	597	34	356	30	677	67	118	19	56	7	991	74	76	38	75	17	1243	112	271	154	111	115	2275	84	442	221	114	106
2012	1588	276	601	35	276	12	760	34	175	11	32	6	905	126	190	48	111	38	1051	117	262	19	118	7	1630	86	515	53	86	81
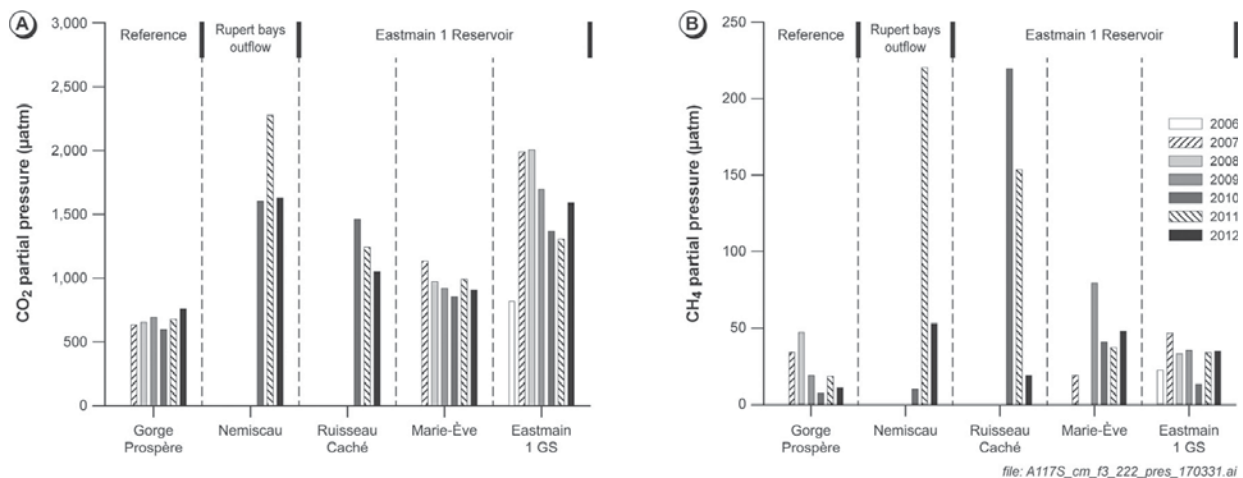
Fig. 3. Averaged CO_2 (A) and CH_4 (B) partial pressures measured by automated systems installed either on rafts at GP (Reference site), NEM (Rupert diversion bays outflow), RC (Eastmain 1 Reservoir downstream NEM), ME (central reservoir) or in Eastmain-1 generating station, from 2006 to 2012. See Table 4, for number of samples and SD.

2010) and 250 µatm (measured in autumn 2011), with an overall average of 106 µatm (SD ± 91). Measurements made at the different sampling stations with AS (GS, ME or GP) showed the same range of partial pressures (Table 4 and Fig. 3), either on the ice-free period, or on the year-round scales. The weak CH_4 concentrations observed and the absence of a trend among seasons and years is certainly linked to methane oxidation in this well oxygenated environment, resulting in pCO_2 increase rather than CH_4, even in ice-cover period (Canelhas et al., 2016).

3.4. Trends in pCO_2 and pCH_4 in the Rupert diversion bays

Partial flooding of the Rupert diversion bays took place in 2009. In August 2010, 90% of the forebay were flooded compared to 50% for the tailbay. The flooding was completed in spring 2011. This sequence is illustrated by the lag in the dissolve gases increases observed between the forebay and the tailbay (Fig. 4A and B). Measurements made in the Rupert Diversion bays during summer field campaigns (around
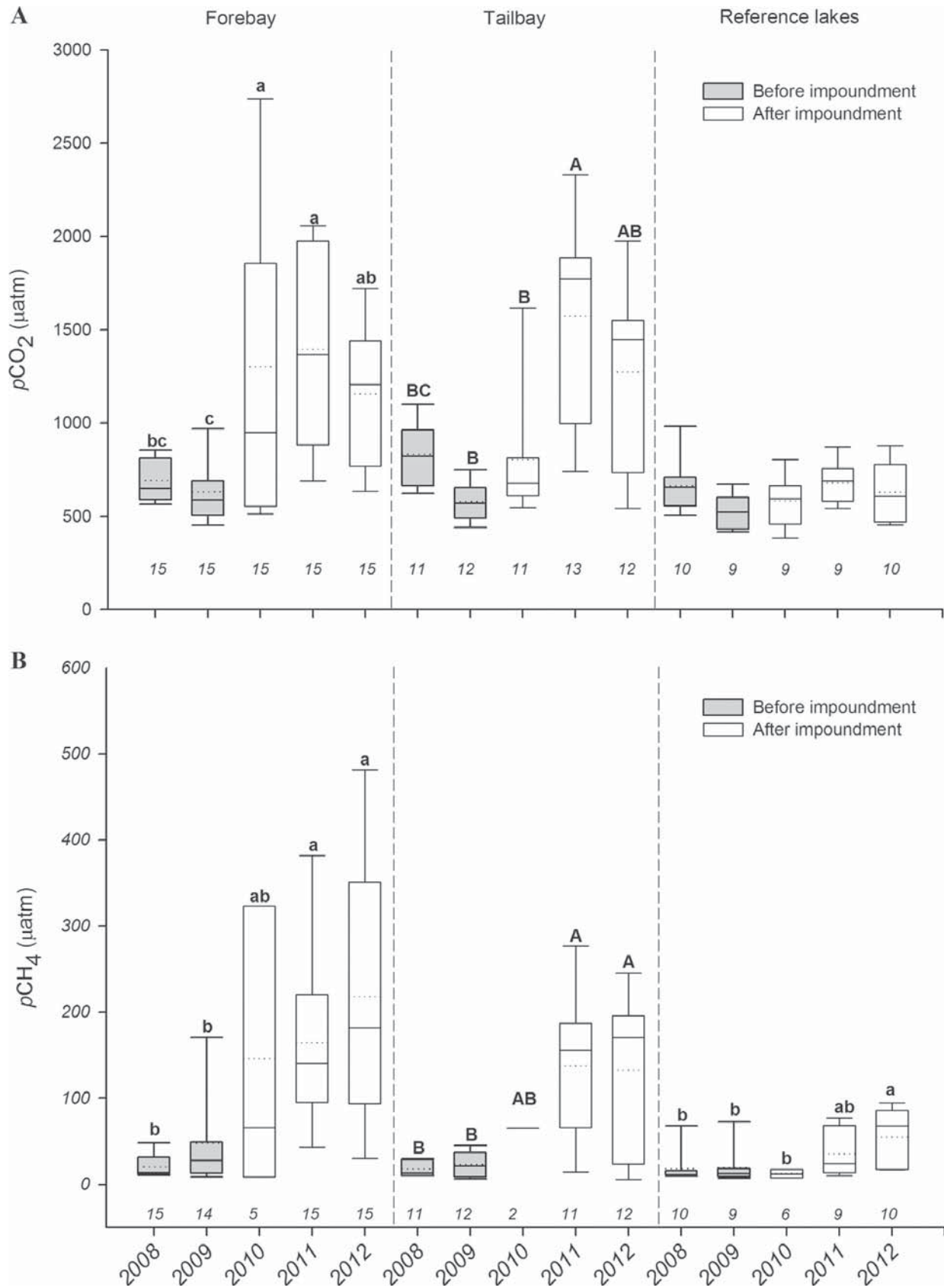
Fig. 4. Averaged CO_2 (A) and CH_4 (B) partial pressures (dotted lines), median (solid lines), 25th and 75th percentiles (boxes), and 10th and 90th percentiles (error bars) measured during field campaigns in the RD bays area between 2008 and 2012. Letters show similar years obtained from a Tukey test (note: no difference for the pCO_2 of the reference lakes). The number of sampled stations (n) is indicated above x-axis of each chart.

35 sampling stations each year) showed that after impoundment, pCO_2 increased significantly (Fig. 4A) but reached values in the range of those observed in Eastmain 1 reservoir since its creation. The averaged pCO_2 for the forebay and tailbay varied from 679 µatm (SD ± 164) before impoundment to 1303 µatm (SD ± 645) for 2010–2011. For the 2008–2009 period, before flooding, the mean pCH_4 was 31 µatm (SD ± 37) for the entire diversion. It increased in 2010 after flooding in the forebay and more significantly in 2011 for the tailbay, reaching a mean value of 138 µatm (SD ± 102), which is higher than what was observed in Eastmain 1 reservoir (Fig. 4b; mean value of 106 µatm presented earlier for Eastmain 1 Reservoir). Both $pCO2$ and pCH_4 were significantly higher than those measured in nearby reference lakes all through the survey, or in the impounded lakes surveyed in 2008 before the diversion. Reference lakes do not show significant trend through the studied years.

3.5. Scale down to the Rupert diversion bays and Eastmain 1 reservoir confluence area

Automated systems installed on rafts at the stations NEM and RC showed high mean pCO_2 and pCH_4 in 2010 and 2011 and a clear drop in 2012 (Fig. 3; Anova and Tukey–Kramer, $p < 0.05$). Table 5 presents mean pCO_2 and pCH_4 measured at the two stations sampled yearly (once per summer; Cache-2 and/or Cache-6; Fig. 1B) in the sediment fan area downstream of the Rupert diversion bays. There is no evidence of pCO_2 increase at these stations after the bays impoundment (2010–2012). In 2010, however, pCH_4 increased by a factor of 30, and then returned to values closer to pre-impoundment pCH_4 in 2011. Different sensors were used in various years but such differences cannot be attributed to variability among them. Once again, the use of AS combined with field campaigns allowed us to capture temporal trends and punctual events.

Overall, pCO_2 recorded at NEM (automated system) were higher than those measured at RC (mean $pCO_2 =$ 1811 µatm ± 560 and mean $pCO_2 = 1234$ µatm ± 315 respectively; T-test, $p < 0.05$). Gas diffusion at the air/water interface along the Rupert derivation bays outlet to the Eastmain 1 reservoir explain the difference observed between these two stations; this phenomenon is currently observed downstream flooded systems (Guérin et al., 2006; Kemenes et al., 2011; Campeau et al., 2014).

Scaling down, in September 2011, 15 stations were sampled for pCO_2 and pCH_4 (Fig. 1B) to better determine the influence of the Rupert diversion on Eastmain 1 reservoir. Stations 1 to 5.5 are considered to be in the sediment fan area; stations 6.5, 10, 11 and 15 are considered a transition zone; stations 14, 16, 12 and 17 are influenced by the Eastmain River water inflow. We found no significant difference between mean pCO_2 measured in these three different areas (Anova and Tukey–Kramer, $p > 0.05$; overall averaged pCO_2: 1347 ± 137 µatm). Mean pCH_4 in the third area (70 µatm; influenced by the Eastmain River) was significantly lower than averaged pCH_4 in the transition area (312 µatm) and the fan area (40 µatm; Anova and Tukey–Kramer, $p < 0.05$).

In conclusion, the impoundment of the Rupert River and the related transport of sediment and organic matter into Eastmain 1 reservoir did not have a significant long term effect on pCO_2 measured in the reservoir.

Systematic sampling conducted in 2011 in the sediment fan area, downstream of the Rupert diversion, clearly showed a gradual dilution of CH_4 in Eastmain 1 reservoir. It thus appears that the CH_4 produced by the Rupert diversion and exported into the reservoir led to a significant increase in CH_4 concentration in the reservoir. The downstream influence of the Rupert diversion is probably due to an export of CH_4, and consequently limited in time (significant drop observed in 2012 by different monitoring methods), rather than to an export of organic matter degraded in the reservoir.

3.6. Eastmain 1 Reservoir CO_2 and CH_4 diffusive emissions

For each field campaign, diffusive emissions were either measured (FC) or estimated (partial pressures and TBL model). Since two different chambers were used during our follow-up, fluxes obtained in 2008 with the first type were analyzed apart. For this period, measured fluxes were significantly lower than estimated fluxes (match pairs T-test, $p < 0.05$; $n = 128$; $y = 0.63x$ and $R^2 = 0.58$). For the subsequent years, there was a strong match between measured and estimated fluxes (match pairs T-test, $p < 0.05$; $n = 338$; $y = 0.89x$ and $R^2 = 0.67$), thus validating the new chamber design. In this section, for presentation purpose only measured fluxes are presented. This decision is supported by consistent methods and because, theoretically, measured fluxes (with FC) are susceptible to be overestimated and thus more conservative.

CO_2 diffusive emissions at the air–water interface ranged between −113 mg C-CO_2 m^{-2} day^{-1} (negative

Table 5

pCO_2 and pCH_4 temporal variations at two stations sampled in summertime in the sediment fan area located downstream of the Rupert diversion.

Date	Water temperature °C	pCO_2 µatm	n	SD	pCH_4 µatm	n	SD
2006-07-11	17	1667	1	N.A.	126	2	17
2007-07-16	15	2066	1	N.A.	N.A.	1	N.A.
2008-07-13	18.9	1081	1	N.A.	57	1	N.A.
2009-07-20	18.1	1221	1	N.A.	174	1	N.A.
2010-07-10	18.4	857	1	N.A.	5135	1	N.A.
2011-08-15	19	1445	2	161	189	2	33
2012-08-01	18	1354	2	51	292	2	123

Table 6
Average ice-free period CO_2 and CH_4 emissions measured in Eastmain 1 reservoir from 2006 to 2012.

Sampling year	CO_2 diffusive emissions				CH_4 diffusive emissions			
	Mean (mgC-CO_2 m^{-2} day^{-1})	n	SD	Tukey test result	Mean (mgC-CH_4 m^{-2} day^{-1})	n	SD	Tukey test result
2006	2223	228	1225	a	7.9	214	9.5	ab
2007	944	101	450	bc	2.4	112	2.6	b
2008	799	240	528	c	N.A.			ab
2009	1100	72	619	bc	N.A.			ab
2010	765	88	584	bc	11.0	87	19.8	a
2011	1021	119	391	bc	11.0	118	13.3	ab
2012	791	91	563	bc	6.3	91	7.7	ab

N.A.: not available.

value corresponding to CO_2 capture) and 8237 mg C-CO_2 m^{-2} day^{-1} measured in 2008 and 2006 respectively. In average, highest emissions were recorded in 2006, after reservoir impoundment and lowest fluxes were measured in 2008 (Table 6; Anova and Tukey–Kramer, $p < 0.05$). CH_4 fluxes ranged from null to 102 mg C-CH_4 m^{-2} day^{-1} measured in 2010. In average, highest CH_4 emission was recorded in 2010, whereas lowest emission was measured in 2007 (Anova and Tukey–Kramer, $p < 0.05$).

In 2012, 6 years and half after the beginning of the reservoir creation, mean CO_2 and CH_4 diffusive emissions were 791 mg C-CO_2 m^{-2} day^{-1} (±563) and 6.3 mg C-CH_4 m^{-2} day^{-1} (±7.7) respectively. In Quebec, overall measurements made in lakes and rivers in the context of GHG emissions studies related to reservoirs (Hydro-Quebec datasets, between 1999 and 2012, $n = 1123$, unpublished results) showed averaged CO_2 emissions of 296 mg C-CO_2 m^{-2} day^{-1} (±359). Eastmain 1 reservoir emissions are thus close to the range of those observed in these systems. According to other studies (Tremblay et al., 2005; Abril et al., 2005) the observed decreasing trend would continue, at a smaller extent, for the three consecutive years (Teodoru et al., 2012). Then, 10 years after flooding, the Eastmain 1 reservoir is expected to behave like a natural lake in terms of diffusive emissions.

3.7. Wintertime respiration rates

Variations in CO_2 concentration in the system were monitored year-round with the AS installed in Eastmain-1 generating station. In winter, the daily pattern presented in Fig. 4 is not observable due to CO_2 accumulation under ice-cover. The heterotrophic activity (Rc) is considered as the main metabolic activity in the reservoir, photosynthesis being reduced by the low light availability under ice-cover (Huner et al., 1998). The difference in CO_2 concentrations at the beginning of the winter and at the peak (just before ice-break-up) and the corresponding number of days (around 165) were used to calculate the daily Rc at the whole reservoir scale. Thereby, decreasing Rc rates were found from winter 2006–2007 to winter 2011–2012, with values ranging respectively from 1.5 to 0.8 μmol L^{-1} day^{-1} (Table 3). This decreasing trend is viewed as the result of the drop in organic matter availability in the reservoir over the years. This pattern was also observed by

Venkiteswaran et al. (2013) in experimental boreal reservoirs.

4. Conclusion

Results presented in this article confirm the predicted CO_2 trend emissions from a boreal reservoir by Teodoru et al. (2012), with a net decrease in the first three years followed by a CO_2 emissions stabilization around seven years after the reservoir creation (see Fig. 2A). The novelty in our article lies in the different methods used to demonstrate this phenomenon, all of them showing the same trend. The present study advocates for long term GHG monitoring (around 10 years). The use of various methods, beforehand intercalibrated, thereby offers a non-negligible flexibility, reducing the sampling costs, which should favor an increase in this kind of studies worldwide. The present study also demonstrates that methane concentrations in the Eastmain 1 Reservoir were very low, did not vary with time after flooding and were not impacted by the flooding of the Rupert diversion bays. In this last area, an increase in methane was observed after flooding; further measurements are planned in 2018 to document the evolution of this phenomenon with time. However, it is hypothesized that methane concentration will reach weak values comparable to those of the Eastmain 1 Reservoir. Thus, our understanding of the studied watersheds tends to demonstrate that methane is not a GHG of concern considering the reservoirs lifetime.

We also demonstrated that the supersaturation in CO_2 observed in the Eastmain 1 Reservoir by the end of winter is supported by the winter respiration and CO_2 accumulation under the water. Year after year, the availability of the leachable and labile organic matter derived from the flooded soils decreases, resulting in lower background pCO_2 for the ice-free period. Finally, we demonstrated that the impoundment of an upstream reservoir had no influence on the metabolism of the Eastmain 1 Reservoir. These results indicate that the flooded soils contribution is negligible after 7 years and that the reservoir effect is over within a 10 years period as predicted by Tremblay et al. (2005).

Conflict of interest

None declared.

Ethical statement

Acknowledgments

Funding body

References

Abril, G., Guérin, F., Richard, S., Delmas, R., Galy-Lacaux, C., Gosse, P., Tremblay, A., Varfalvy, L., Aurelio Dos Santos, M., Matvienko, B., 2005. Carbon dioxide and methane emissions and the carbon budget of a 10-year-old tropical reservoir (Petit-Saut, French Guiana). Glob. Biogeochem. Cycles 19, GB4007, http://dx.doi.org/10.1029/2005GB002457.

Barros, N., Cole, J.J., Tranvik, L., Prairie, Y.T., Bastviken, D., Huszar, V.L.M., del Giorgio, P., Roland, F., 2011. Carbon emission from hydroelectric reservoirs linked to reservoir age and latitude. Nat. Geosci. 4, 593–596.

Bastien, J., Gravel, R., Demarty, M., Smith, M., Gill, R., 2010. Reservoir Greenhouse Gas Monitoring Report – 2008–2009 Report prepared by Environnement Illimité inc. for Manitoba Hydro, 111 p. and 1 appendix.

Berggren, M., Lapierre, J.F., del Giorgio, P.A., 2012. Magnitude and regulation of bacterioplankton respiratory quotient across freshwater environmental gradients. ISMEJ 6, 984–993.

Campeau, A., Lapierre, J.-F., Vachon, D., del Giorgio, P.A., 2014. Regional contribution of CO_2 and CH_4 fluxes from the fluvial network in a lowland boreal landscape of Québec. Glob. Biogeochem. Cycles 28 , http://dx.doi.org/10.1002/2013GB004685.

Canelhas, M.R., Denfeld, A.B.A., Weyhenmeyer, G.A., Bastviken, D., Bertilsson, S., 2016. Methane oxidation at the water-ice interface of an ice-covered lake. Limnol. Oceanogr. 61, S78–S90.

Clayer, F., Gobeil, C., Tessier, A., 2016. Rates and pathways of sedimentary organic matter mineralization in two basins of a boreal lake: emphasis on methanogenesis and methanotrophy. Limnol. Oceanogr., http://dx.doi.org/10.1002/lno.10323.

Cole, J.J., Prairie, Y.T., Caraco, N.F., McDowell, W.H., Tranvik, L.J., Striegl, R.G., Duarte, C.M., Kortelainen, P., Downing, J.A., Middelburg, J.J., Melack, J., 2007. Plumbing the global carbon cycle: integrating inland waters into the terrestrial carbon budget. Ecosystems 10, 172–185.

Del Giorgio, P.A., Cole, J.J., Caraco, N.F., Peters, R.H., 1999. Linking planktonic biomass and metabolism to net gas fluxes in northern temperate lakes. Ecology 80, 1422–1431.

DelSontro, T., McGinnis, D.F., Sobek, S., Ostrovsky, I., Wehrli, B., 2010. Extreme methane emissions from a Swiss hydropower reservoir: contribution from bubbling sediments. Environ. Sci. Technol. 44, 2419–2425.

Demarty, M., Bastien, J., Tremblay, A., Hesslein, R., Gill, R., 2009. Greenhouse gas emissions from Boreal Reservoirs in Manitoba and Québec, Canada, measured with automated systems. Environ. Sci. Technol. 43, 8908–8915.

Demarty, M., Bastien, J., 2011. GHG emissions from hydroelectric reservoirs in tropical and equatorial regions: review of 20 years of CH_4 emission measurements. Energy Policy 29, 4197–4206.

Demarty, M., Bastien, J., Tremblay, A., 2011. Annual follow-up of gross diffusive carbon dioxide and methane emissions from a boreal reservoir and two nearby lakes in Québec, Canada. Biogeosciences 8, 41–53.

Deshmukh, C., Serça, D., Delon, C., Tardif, R., Demarty, M., Jarnot, C., Meyerfeld, Y., Chanudet, V., Guédant, P., Rode, W., Descloux, S., Guérin, F., 2014. Physical controls on CH_4 emissions from a newly flooded subtropical freshwater hydroelectric reservoir: Nam Theun 2. Biogeosciences 11, 4251–4269.

Duarte, C.M., Prairie, Y.T., 2005. Prevalence of heterotrophy and atmospheric CO_2 emissions from aquatic ecosystems. Ecosystems 8, 862–8705.

Eggleston, H.S., Buendia, L., Iwa, K., Ngara, T., Tanabe, K., 2006. Intergovernmental Panel on Climate Change (IPCC), National Greenhouse Gas Inventory Guidelines, Vol. 4 – Agriculture, Forestry and Other Land Use. IGES, Kanagawa, Japan, pp. AP2.1–AP2.9.

Guérin, F., Abril, G., Richard, S., Burban, B., Reynouard, C., Seyler, P., Delmas, R., 2006. Methane and carbon dioxide emissions from tropical reservoirs: significance of downstream rivers. Geophys. Res. Lett. 33, L21407.

Huner, N.P.A., Öquist, G., Sarhan, F., 1998. Energy balance and acclimation to light and cold. Trends Plant Sci. 3 (6), 224–230.

Huttunen, J.T., Hammar, T., Manninen, P., Servomaa, K., Martikainen, P.J., 2004. Potential springtime greenhouse gas emissions from a small southern boreal lake (Keihäsjärvi, Finland). Boreal Environ. Res. 9, 421–427.

Huttunen, J.T., Alm, J., Liikanen, A., Juutinen, S., Larmola, T., Hammar, T., Silvola, J., Martikainen, P.J., 2003. Fluxes of methane, carbon dioxide and nitrous oxide in boreal lakes and potential anthropogenic effects on the aquatic greenhouse gas emissions. Chemosphere 52, 609–621.

Kemenes, A., Forsberg, B.R., Melack, J.M., 2011. CO_2 emissions from a tropical hydroelectric reservoir (Balbina, Brazil). J. Geophys. Res. 116, G03004, http://dx.doi.org/10.1029/2010JG001465.

Kling, G.W., Kipphut, G.W., Miller, M.C., 1992. The flux of CO_2 and CH_4 from lakes and rivers in arctic Alaska. Hydrobiologia 240, 23–36.

Kortelainen, P., Huttunen, J.T., Väisänen, T., Mattsson, T., Karjalainen, P., Martikainen, P.J., 2000. CH_4, CO_2 and N_2O supersaturation in 12 Finnish lakes before and after ice-melt. Verh. Int. Verein Limnol. 27, 1410–1414.

Lindsey, R., 2009. Climate and Earth's Energy Budget. http://earthobservatory.nasa.gov/Features/EnergyBalance.

MacIntyre, S., Wanninkhof, R., Chanton, J.P., 1995. Trace gas exchange across the air-water interface in freshwater and costal marine environments. In: Matson, P.A., Harris, R.C. (Eds.), Biogenic Trace Gases: Measuring Emissions from Soil and Water. Blackwell Science, Cambridge, MA, pp. 52–97.

Marchand, D., Demarty, M., Tremblay, A., 2012. Aménagement hydro-électrique de l'Eastmain-1 – Étude des flux de gaz à effet de serre – Résultats été Joint report prepared by Environnement Illimité inc. and Hydro-Québec Production, Direction Gestion des actifs et conformité réglementaire. 46 pages and 1 appendix.

Marchand, D., Prairie, Y.T., Del Giodio, P.A., 2009. Linking forest fires to lake metabolism and carbon dioxide emissions in the boreal region of Northern Québec. Glob. Change Biol. 15, 2861–2873, http://dx.doi.org/10.1111/j.1365-2486.2009.01979.

National Energy Board, 2010. http://www.neb-one.gc.ca.

Planas, D., Paquet, S., Saint Pierre, A., 2005. Production-consumption of CO_2 in reservoirs and lakes in relation to plankton metabolism. In: Tremblay, A., Varfalvy, L., Roehm, C., Garneau, M. (Eds.), Greenhouse Gas Emissions: Fluxes and Processes, Hydroelectric Reservoirs and Natural Environments. Springer-Verlag, Berlin, Heidelberg/New York, pp. 483–503.

Roehm, C., Tremblay, A., 2006. Role of turbines in carbon dioxide emissions from two boreal reservoirs, Québec, Canada. J. Geophys. Res. 111, D24101, http://dx.doi.org/10.1029/2006JD007292.

Rosa, L.P., Matvienko, B., Santos, M.A., Sikar, E., Xavier, A.E., Santos, E., Menezes, C.F., Luorenço, R.S.M., 2002. Carbon dioxide and methane emissions from Brazilian hydroelectric reservoirs: Background report. Brazilian Ministry of Science and Technology. www.mct.gov.br/clima.

Rudd, J.W.M., Harris, R., Kelly, C.A., Hecky, R.E., 1993. Are hydroelectric reservoirs significant sources of greenhouse gases? Ambio 22, 246–248.

St Louis, V., Kelly, C.A., Duchemin, E., Rudd, J.W.M., Rosenberg, D.M., 2000. Reservoir surfaces as sources of greenhouse gases to the atmosphere: a global estimate. BioScience 50 (9), 766–775.

Teodoru, C.R., Bastien, J., Bonneville, M.-C., del Giorgio, P.A., Demarty, M., Garneau, M., Hélie, J.-F., Pelletier, L., Prairie, Y.T., Roulet, N.T., Strachan, I.B., Tremblay, A., 2012. The net carbon footprint of a newly created boreal hydroelectric reservoir. Glob. Biogeochem. Cycles 26 .

Tremblay, A., Therrien, J., Hamelin, B., Wichmann, E., LeDrew, L.J., 2005. GHG emissions from boreal reservoirs and natural aquatic ecosystems. In: Tremblay, A., Varfalvy, L., Roehm, C., Garneau, M. (Eds.), Greenhouse Gas Emissions: Fluxes and Processes, Hydroelectric Reservoirs and Natural Environments. Springer-Verlag, Berlin, Heidelberg/New York, pp. 209–231.

UNESCO/IHA, 2010. In: Goldenfum, J.A. (Ed.), GHG Measurement Guidelines for Freshwater Reservoirs. UNESCO/IHA, London.

Vachon, D., Prairie, Y.T., 2013. The ecosystem size and shape dependence of gas transfer velocity versus wind speed relationships in lakes. Can. J. Fish. Aquat. Sci. 70, 1757–1764.

Vachon, D., Prairie, Y.T., Cole, J.J., 2010. The relationship between near-surface turbulence and gas transfer velocity in freshwater systems and its implications for floating chamber measurements of gas exchange. Limnol. Oceanogr. 55 (4), 1723–1732.

Venkiteswaran, J.J., Schiff, S.L., St. Louis, V.L., Matthews, C.J.D., Boudreau, N.M., Joyce, E.M., Beaty, K.G., Bodaly, R.A., 2013. Processes affecting greenhouse gas production in experimental boreal reservoirs. Glob. Biogeochem. Cycles 27, 567–577, http://dx.doi.org/10.1002/gbc.20046.

Zhao, Y., Sherman, B., Ford, P., Demarty, M., Del Sontro, T., Harby, A., Tremblay, A., Øverjordet, I.B., Zhao, X., Hansen, B.H., Wu, B., 2015. A comparison of methods for the measurement of CO_2 and CH_4 emissions from surface water reservoirs: results from an international workshop held at Three Gorges Dam, June 2012. Limnol. Oceanogr. Methods 13, 15–29.